sustainability

MDPI

Article

Effects of Biochar Application on Soil Water, Heat, and Salt Transport and Rice Growth in Paddy Fields

Xuexiu Huang [1], Ennan Zheng [1,*], Zijia Feng [2,*], Zhijuan Qi [3] and Huiling Tong [4]

[1] School of Hydraulic and Electric Power, Heilongjiang University, Harbin 150080, China; 2251901@s.hlju.edu.cn
[2] Heilongjiang Province Hydraulic Research Institute, Harbin 150080, China
[3] School of Water Conservancy and Civil Engineering, Northeast Agricultural University, Harbin 150030, China; zhijuan.qi@neau.edu.cn
[4] Hangzhou Hydropower Construction Group Co., Ltd., Hangzhou 311228, China; 15293500463@163.com
* Correspondence: 2020024@hlju.edu.cn (E.Z.); zen_hlj@163.com (Z.F.)

Abstract

Seasonal freeze–thaw processes may alter soil water, temperature, and salinity conditions in cold-region paddy fields, potentially affecting rice growth. However, the responses of soil conditions and rice growth to different biochar application rates remain unclear. A field experiment was conducted in Heilongjiang Province, China, with four biochar application rates (0, 5, 10, and 15 t ha^{-1}). Soil moisture, temperature, and salinity were monitored at different depths, while rice root morphology, agronomic traits, dry biomass, and photosynthetic parameters were measured. The overall effects were assessed using the logarithmic percentage change-driven objective weighting (LOPCOW) and stable preference ordering towards ideal solution (SPOTIS) methods. Compared with the control, the 10 and 15 t ha^{-1} treatments increased mean soil moisture by 4.26–21.10% and 5.83–25.21%, respectively. The 5 t ha^{-1} treatment reduced mean soil salinity by 52.81–70.98%, whereas the 10 t ha^{-1} treatment increased salinity at 80–100 cm. Soil temperature fluctuations decreased with depth. At the heading and flowering stage, total root length increased by 23.14–34.47% under biochar treatments compared with the control, with the greatest increase observed at 10 t ha^{-1}. No significant differences in net photosynthetic rate were observed among treatments at the heading and flowering stage. At the milk-ripe stage, aboveground dry biomass increased by 14.04% under the 15 t ha^{-1} treatment compared with the control. The LOPCOW–SPOTIS assessment ranked the treatments as 15 > 10 > 5 > 0 t ha^{-1}. These findings highlight the application-rate-dependent responses of soil conditions and rice growth, providing insights into biochar management in cold-region paddy fields.

Keywords: biochar; water, heat, and salt transport; rice growth; LOPCOW–SPOTIS integrated assessment

Academic Editors: Rosa Rodriguez, Germán Mazza and María Paula Fabani

Received: 29 October 2026
Revised: 19 November 2026
Accepted: 25 November 2026
Published: 28 November 2026

Copyright: © 2026 by the authors. Licensee MDPI, Basel, Switzerland. This article is an open access article distributed under the terms and conditions of the Creative Commons Attribution (CC BY) license.

1. Introduction

The distribution and dynamics of soil moisture, heat, and salts collectively influence the root-zone environment and play important roles in crop growth and agricultural productivity. Water movement serves as the primary carrier of salt transport, while temperature variations affect water and salt redistribution by regulating evaporation, heat transfer, and water phase transitions. Under alternating irrigation and evaporation

conditions, salts can be leached downward with infiltrating water or transported upward through capillary flow. The location and extent of salt accumulation directly affect soil conditions in the root zone [1]. Excessive salt accumulation can induce osmotic stress and ion toxicity, restrict root water uptake, and disrupt ionic homeostasis in plants, thereby inhibiting leaf growth and biomass accumulation [2]. Cold-region paddy fields also undergo seasonal freeze–thaw cycles, which can alter soil pore structure, hydraulic properties, and hydrothermal distribution, thereby affecting soil water retention and movement after winter [3–5]. Biochar is a carbon-rich material produced through the pyrolysis of biomass under oxygen-limited or oxygen-free conditions. Its porous structure and surface properties provide a basis for regulating soil water and solute distribution. Once incorporated into soil, biochar can retain water within its internal pores and influence water infiltration, retention, and release by reducing soil bulk density and modifying interparticle pore distribution. However, these effects depend on both biochar properties and soil texture [6,7]. Changes in soil moisture further influence salt dissolution and transport, while temperature variations contribute to water and salt redistribution by affecting evaporation, heat transfer, and phase transitions. Therefore, biochar-induced changes in soil water movement may alter salt distribution within the soil profile and the water, temperature, and salinity conditions in the rice root zone. These changes may subsequently affect root development, water and nutrient uptake, and leaf photosynthetic activity, thereby influencing aboveground growth and dry matter accumulation in rice. Thus, biochar-induced changes in paddy soil conditions may be associated with rice growth responses.

The effects of biochar on soil conditions involve multiple processes, including water retention, heat transfer, and salt redistribution. Irrigation water quality and biochar application rate can influence the extent to which biochar regulates soil evaporation and water retention [8,9]. Biochar-induced changes in soil bulk density and composition can also affect thermal conductivity and diffusivity, thereby altering soil heat transfer [10]. These changes in soil moisture and structure may further influence salt leaching and redistribution within the soil profile, with their effects also depending on irrigation water quality and the combined application of other soil amendments [11]. Soil water and salt responses also vary with biochar application methods. For example, soil column experiments have shown that a biochar interlayer can reduce evaporation and inhibit upward salt transport to the soil surface [12]. Previous studies have demonstrated the potential of biochar to improve salt-affected soils, although its effectiveness varies with initial soil salinity, biochar feedstock, application rate, and soil conditions [13,14]. Whether improvements in soil conditions translate into enhanced crop growth also depends on the responses of root development and aboveground physiological processes. Long-term field experiments in paddy soils have shown that biochar can regulate rice root development across growth stages, improve soil conditions, and reduce nitrogen leaching when combined with nitrogen fertilization, highlighting the joint contributions of root development and soil conditions to rice productivity [15]. Studies conducted in saline–alkaline paddy fields have also shown that biochar can improve ionic homeostasis and alleviate physiological stress in rice, thereby promoting grain filling and yield formation [16]. However, rice growth and yield responses depend on biochar properties, application rate, and water and fertilizer management practices [17]. Collectively, these studies provide insights into the agricultural effects of biochar while highlighting their dependence on specific environmental and management conditions, underscoring the need for further validation under local field conditions.

The effects of biochar on soil conditions and rice growth in cold-region paddy fields subjected to seasonal freeze–thaw cycles remain insufficiently understood. Previous studies have demonstrated that biochar can improve soil conditions by influencing water retention, heat transfer, and salt redistribution. However, these effects depend on biochar

properties, soil type, climatic conditions, and field management practices, leading to variations in findings across regions and experimental settings [18,19]. Consequently, existing evidence remains insufficient to determine how biochar affects the vertical distribution of soil moisture, temperature, and salinity in cold-region paddy fields following seasonal freeze–thaw cycles when incorporated into soil by rotary tillage. Furthermore, biochar may alter the vertical transport and redistribution of soil water and salts, meaning that improvements in surface soil conditions do not necessarily correspond to reduced salinity throughout the entire soil profile [20]. Therefore, soil moisture, temperature, and salinity at different depths should be jointly considered to comprehensively assess the effects of biochar on soil conditions. Furthermore, the extent to which changes in soil conditions benefit rice growth depends on root development and aboveground physiological responses. Previous studies have shown that increasing biochar application rates does not necessarily lead to greater improvements in rice yield [21], while the effects of biochar on rice root growth and resource utilization are also influenced by factors such as water management [22]. However, integrated analyses of changes in soil moisture, temperature, and salinity profiles alongside rice root and aboveground growth responses remain limited. Moreover, differences in soil improvement and rice growth among biochar application rates cannot be fully captured by individual indicators. Therefore, field investigations in cold-region paddy fields are needed to systematically examine soil and crop responses to different biochar application rates by integrating soil moisture, temperature, and salinity profile measurements with multiple rice growth indicators, followed by a multi-criteria assessment.

Accordingly, this study was conducted in cold-region paddy fields in Qing'an County, Heilongjiang Province, China, with four biochar application rates (0, 5, 10, and 15 t ha^{-1}) to investigate their effects on soil conditions and rice growth. Given the differences in measurement units, indicator directions, and evaluation purposes among soil moisture, temperature, salinity, root morphological traits, agronomic traits, and photosynthetic parameters, individual indicators cannot fully reflect the overall effects of biochar application. Therefore, the logarithmic percentage change-driven objective weighting (LOPCOW) method was used to determine objective indicator weights, while the stable preference ordering towards ideal solution (SPOTIS) method was employed to calculate the weighted normalized distances between each treatment and a predefined ideal solution, enabling a multi-criteria evaluation. Three hypotheses were proposed: (1) biochar application at different rates may alter the vertical distribution of soil moisture, temperature, and salinity in cold-region paddy fields, with effects varying across soil depths rather than consistently increasing with application rate; (2) changes in soil moisture, temperature, and salinity conditions may be associated with rice root morphology, agronomic traits, and photosynthetic responses, resulting in different growth responses among treatments; and (3) different biochar application rates may offer distinct advantages in improving soil conditions and promoting rice growth, allowing treatments with better overall performance to be identified through a multi-criteria evaluation. To test these hypotheses, changes in soil moisture, temperature, and salinity at different depths were monitored during the rice growing season following seasonal freeze–thaw cycles. Responses in rice root development, agronomic traits, photosynthetic parameters, and dry matter accumulation were also examined. The LOPCOW–SPOTIS method was then applied to evaluate the overall performance of each treatment, providing a reference for appropriate biochar application in cold-region paddy fields.

2. Materials and Methods

2.1. Study Site Description

The field experiment was conducted at the Qing'an National Key Irrigation Experimental Station, located in Heping Town, Qing'an County, Heilongjiang Province, China (46°57′28″ N, 127°40′45″ E), within the cold-region black soil zone. The region has a cold-temperate continental monsoon climate, with a frost-free period of 128 d, a crop growing season of 156–171 d, and a long-term mean open-water evaporation of 750 mm. The experimental field consisted of black soil-derived paddy soil that had been cultivated with rice for more than 20 years. The initial soil pH was 6.42. In the 0–20 cm cultivated layer, the soil contained 41.7 g kg^{-1} organic matter, 1.52 g kg^{-1} total nitrogen, 15.26 g kg^{-1} total phosphorus, 19.85 g kg^{-1} total potassium, 148.36 mg kg^{-1} alkali-hydrolyzable nitrogen, 24.25 mg kg^{-1} available phosphorus, and 156.22 mg kg^{-1} available potassium. The saturated soil moisture content was 34.12%. The biochar used in this study was produced from rice straw by pyrolysis at 500 °C for 2 h under anaerobic conditions. Its main physicochemical properties were as follows: a specific surface area of 81.85 m^2 g^{-1}, pH of 8.75, organic carbon content of 41.05%, nitrogen content of 1.13%, bulk density of 0.12 g cm^{-3}, cation exchange capacity of 42.09 cmol kg^{-1}, packing density of 0.12 g cm^{-3}, and total pore volume of 0.09 cm^3 g^{-1}.

2.2. Experimental Design

The experiment was conducted from November 2025 to October 2026. Biochar was applied once in autumn 2025 before soil freezing. It was uniformly spread over the soil surface and subsequently thoroughly incorporated into the soil using a rotary tiller. No additional biochar was applied during the experimental period. Four biochar application rates (0, 5, 10, and 15 t ha^{-1}) were established in the field experiment, designated as B0, B1, B2, and B3, respectively. B0 served as the control without biochar application, while B1, B2, and B3 represented low, medium, and high application rates, respectively. The application rates were selected based on ranges reported in previous studies of biochar application in paddy fields, while considering the field conditions and the need for comparisons across application rates. This design aimed to investigate the effects of different biochar application rates on soil moisture, temperature, salinity, and rice growth, providing a basis for identifying suitable application rates in cold-region paddy fields [23]. Each treatment was replicated three times, resulting in 12 experimental plots, each measuring 100 m^2 (10 m × 10 m). The plots were arranged in a randomized complete block design. To prevent the lateral movement of water and nutrients between adjacent plots, plastic barriers were installed vertically to a depth of 40 cm beneath the bunds separating the plots.

The application rates and timing of nitrogen, phosphorus, and potassium fertilizers followed local fertilization guidelines. Controlled irrigation was applied uniformly across all treatments, with water management adjusted according to the water requirements of rice at different growth stages. During the regreening stage, a standing water depth of 0–30 mm was maintained. During the early and middle tillering stages, the lower soil moisture threshold was set at 70% of the saturated soil moisture content in the root zone, with a maximum standing water depth of 30 mm. At late tillering, the fields were drained and allowed to dry. During jointing and heading, the lower soil moisture threshold was increased to 80% of the saturated soil moisture content, while the maximum standing water depth remained at 30 mm. At the milk-ripe stage, the lower threshold was set at 70% of the saturated soil moisture content, with no standing water maintained. The fields were allowed to dry naturally at maturity. Except during regreening, fertilization, pesticide application, temporary rainwater storage (a standing water depth of 3 cm for no more than 5 d), and the yellow-ripening stage, no standing water was maintained. Irrigation and

drainage were regulated according to soil moisture content in the rice root zone. Irrigation was initiated when soil moisture content fell below the specified lower threshold, and excess water was drained when the prescribed upper limit was exceeded.

Nitrogen (N) was applied at an annual rate of 110 kg ha^{-1} as urea (46% N), with basal, tillering, and panicle fertilizers applied at a ratio of 5:2:3. Potassium (K_2O) was applied at 80 kg ha^{-1} as potassium chloride (60% K_2O), divided equally between basal application and the 8.5-leaf stage (panicle initiation). Phosphorus (P_2O_5) was applied at 45 kg ha^{-1} as diammonium phosphate (46% P_2O_5) in a single basal application. A locally predominant rice cultivar was used, following the conventional local planting pattern with a plant and row spacing of 3 cun × 10 cun (approximately 10 cm × 33.3 cm). A buffer zone was maintained along the boundaries of each experimental plot, where no rice was planted, resulting in an actual planting density of 24 hills m^{-2}, with three seedlings per hill. To ensure comparability among treatments, the same planting pattern and density were maintained across all treatments, minimizing potential interference from differences in planting density when evaluating the effects of biochar application. Other cultivation practices, including seedling raising, transplanting, pest and disease management, and pesticide application, followed conventional local agricultural practices.

2.3. Sample Collection and Measurement Methods

Agronomic Traits

Three rice plants were randomly selected from each experimental plot for root sampling. To preserve root integrity, whole plants were carefully excavated with a shovel to a depth of 80 cm. The roots were gently shaken to remove loose soil while minimizing root damage. After excavation, the shoots were separated from the roots, which were then placed in 200-mesh nylon bags. The roots were subsequently placed on a sieve with a mesh opening of 0.5 mm and gently rinsed with tap water to remove adhering soil while minimizing fine-root loss. Dead and decayed root fragments were manually removed. Immediately after washing, the roots were scanned at a resolution of 300 dots per inch (dpi) using an EPSON 12000XL scanner (Seiko Epson Corporation , Suwa, Japan). The images were then analyzed using WinRHIZO Pro 2023a root analysis software (Regent Instruments Inc., Canada) to determine total root length, mean root diameter, root surface area, and root volume.

After seedling emergence, nine rice plants with uniform growth were selected and tagged in each experimental plot. Plant height was measured using a measuring tape, leaf area was determined using a leaf area meter (LI-3000C, Beijing Ecotek Technology Co., Ltd., Beijing, China), and tiller number was recorded during the tillering stage. In addition, net photosynthetic rate (Pn), stomatal conductance (Gs), intercellular CO_2 concentration (Ci), and transpiration rate (Tr) were measured at different growth stages using a portable photosynthesis system (LI-6400XT, LI-COR Biosciences, Lincoln ,USA).

At each growth stage from the regreening stage to the milk-ripe stage, rice plants from six hills with uniform growth were sampled from each experimental plot. The plants were separated into roots, stems and sheaths, leaves, and panicles (after heading). The samples were placed in separate bags, heated at 105 °C for 30 min to inactivate enzymes, and subsequently oven-dried at 80 °C to constant weight. The dry weight of each plant component was determined using an electronic balance with a precision of 0.01 g.

At rice maturity, five sampling locations were selected from each experimental plot using a five-point sampling method. A 1 m^2 sampling area was established at each location, excluding border rows. The number of effective panicles per unit area was recorded, and grain yield was determined by manual harvesting, threshing, sun-drying, and weighing. In addition, five representative rice hills were randomly selected from each plot to assess yield components. After threshing, filled and unfilled grains were separated and counted

to calculate the mean number of grains per panicle and the seed-setting rate. The harvested grains were subsequently placed in paper envelopes and oven-dried at 60 °C to constant weight. The mean thousand-grain weight was then determined using an electronic balance.

Soil temperature was monitored throughout the rice growing season, from transplanting to harvest, using soil temperature sensors (HZTJ1-1). Monitoring locations were selected on relatively level ground within each experimental plot to minimize the influence of surface irregularities. Soil temperature was measured at depths of 0, 10, 20, 30, and 40 cm at regular intervals. Soil samples were collected, sealed in plastic bags, and transported to the laboratory, where they were air-dried, crushed, and sieved. Soil extracts were prepared at a soil-to-water ratio of 1:5, and their electrical conductivity ($EC_{1:5}$) was measured using a DDS-307 conductivity meter (Shanghai INESA Scientific Instrument Co., Ltd., Shanghai, China). Soil salinity was subsequently calculated based on the relationship between electrical conductivity and soil salt content [24].

Soil moisture content was determined using the oven-drying method. Fresh soil samples were placed in aluminum containers and weighed before drying. The samples were then oven-dried at 105 °C for at least 8 h and weighed again to determine their dry mass. Gravimetric soil moisture content was calculated as the difference between the wet and dry soil masses divided by the dry soil mass.

2.4. Data Processing Methods

To comprehensively evaluate the effects of different biochar treatments on paddy soil conditions and rice growth, a multi-criteria evaluation framework was established using 16 indicators across four categories: soil moisture, temperature, and salinity; root characteristics; growth traits; and photosynthetic traits (Table 1). Data from relevant observation periods were selected based on the growth-stage variations in each indicator and the experimental monitoring schedule [25,26]. After normalization, indicator weights were determined using the LOPCOW method [27], and the weighted normalized distance between each treatment and the ideal solution was calculated using the SPOTIS method [28]. These distances were then converted into overall scores.

Table 1. Indicator framework for the integrated assessment of effects on paddy soil conditions and rice growth.

Goal Layer	Category	Indicator	Indicator Direction
Comprehensive effects on paddy soil conditions and rice growth	Soil water, temperature and salinity	Soil water content	Optimum-type
		Soil salinity	Negative
		Soil temperature variability	Negative
	Root characteristics	Total root length	Positive
		Total root surface area	Positive
		Root volume	Positive
		Root diameter	Optimum-type
	Growth traits	Leaf area	Positive
		Plant height	Positive
		Tiller number	Positive
		Aboveground dry biomass	Positive
		Grain weight	Positive
	Photosynthetic traits	Net photosynthetic rate	Positive
		Transpiration rate	Optimum-type
		Stomatal conductance	Optimum-type
		Intercellular CO_2 concentration	Optimum-type

1. Indicator Normalization

Indicators were normalized according to their orientations using benefit-type, cost-type, and target-type normalization methods [29]. For target-type indicators, the mean value across treatments was used as the reference point, and normalization was performed based on the deviation of each indicator value from this mean [30]. This approach enabled relative comparisons among treatments by reflecting the overall distribution of indicator values under the experimental conditions. Notably, the treatment mean served only as a reference for relative evaluation and did not represent the actual physiological or agronomic optimum.

$$y_{ij} = \begin{cases} \frac{x_{ij}-x_{j,min}}{x_{j,max}-x_{j,min}}, & \text{(Positive)} \\ \frac{x_{j,max}-x_{ij}}{x_{j,max}-x_{j,min}}, & (Negative) \\ 1-\frac{|x_{ij}-\bar{x}_j|}{\max(x_{j,max}-\bar{x}_j,\bar{x}_j-x_{j,min})}, & \text{(Optimum-type)} \end{cases}, \quad (1)$$

where x_{ij} is the original value of indicator j for treatment i; $x_{j,max}$, $x_{j,min}$, and $\bar{x}_j$ are the maximum, minimum, and mean values, respectively, of indicator j across the four treatments; and y_{ij} is the normalized value. After normalization, all indicators were expressed on a common assessment scale of [0, 1], with higher values indicating greater alignment with the assessment objectives. For target-type indicators, the mean was used as the central reference value for relative assessment and did not represent a physiological optimum.

2. Indicator Weighting Using LOPCOW

The logarithmic percentage value of each indicator was calculated from the normalized data, and these values were then normalized to obtain the indicator weights [31]:

$$PV_j = 100\left|\ln\left(\frac{\sqrt{\frac{1}{m}\sum_{i=1}^{m} y_{ij}^2}}{\sigma_j}\right)\right|, \quad (2)$$

$$w_j = \frac{PV_j}{\sum_{k=1}^{n} PV_k}, \quad (3)$$

where PV_j is the logarithmic percentage value of indicator j; σ_j is the population standard deviation of its normalized values, calculated using the number of treatments, m, as the denominator in the variance calculation; and w_j is the weight of indicator j, with all indicator weights summing to 1. In this study, m = 4 and n = 16. The weight of each category was calculated as the sum of the weights of its constituent indicators.

3. Integrated Assessment Using SPOTIS

The weighted normalized distance between each treatment and the ideal state was calculated as follows:

$$D_i = \sum_{j=1}^{n} w_j \frac{|y_{ij}-y_j^*|}{|U_j-L_j|}, \quad (4)$$

where D_i is the overall distance for treatment i; y_j^* is the ideal value of indicator j; and U_j and L_j are the predefined upper and lower bounds of indicator j, respectively. In this study, normalized values were used as inputs, with $L_j = 0$ and $U_j = 1$, and $y_j^* = 1$ for all indicators.

To facilitate comparison, the overall distance was converted into an overall score as follows:

$$S_i = 1 - D_i. \quad (5)$$

where S_i is the overall score for treatment i. A smaller overall distance and a higher overall score indicate better overall treatment performance. The treatments were ranked in descending order of their overall scores [32].

In addition, sensitivity analysis was conducted under different evaluation scenarios by adjusting indicator weights and the normalization reference values for target-type indicators to assess the robustness of the overall evaluation results.

3. Results

3.1. Effects of Biochar Application Rates on Rice Root Characteristics

Rice root characteristics generally increased and then decreased across growth stages under different biochar treatments, with all parameters except total root length reaching relatively high values at the heading and flowering stage (Figure 1). At the heading and flowering stage, total root length increased by 23.14%, 34.47%, and 28.92% under the B1, B2, and B3 treatments, respectively, compared with the control (B0), with the greatest increase observed under the B2 treatment. Root surface area increased by 14.30%, 9.10%, and 4.44%, respectively, with a significant increase observed only under B1 ($p < 0.05$). Root volume increased by 1.20%, 1.20%, and 12.37%, respectively, with a significant increase observed only under B3 ($p < 0.05$). In contrast, mean root diameter decreased by 4.76%, 6.80%, and 4.76%, respectively, although none of these differences were significant ($p > 0.05$). Across the growing season, B2 showed the greatest increase in total root length, followed by B3 and B1, whereas B1 exhibited the strongest positive response in root surface area during the later growth stages. B3 generally showed greater root volume during the early growth stages and from jointing and booting to heading and flowering, while B1 and B2 performed relatively better during the middle and late tillering stages. Differences in root volume among treatments narrowed at the milk-ripe stage. For mean root diameter, B0 generally showed higher values before tillering and at heading and flowering, whereas B2 showed relatively higher values during jointing and booting. B1 remained comparable to B0, while B3 generally exhibited smaller root diameters. Differences in root diameter among treatments diminished during the later growth stages.

3.2. Effects of Biochar Application Rates on Rice Agronomic Traits

Figure 2 illustrates the dynamic changes in rice agronomic traits and aboveground dry matter accumulation under different biochar treatments. Tiller number generally increased and then decreased across growth stages, with no significant differences among treatments. B0 and B2 reached peak values of 32 and 29 tillers, respectively, before declining to 19 and 20. Similarly, B1 increased to 28 tillers before decreasing to 18, while B3 reached 27 tillers and subsequently fluctuated slightly before declining to 19. Tiller numbers gradually converged among treatments during the later growth stages. Plant height and aboveground dry matter increased progressively across growth stages, reaching their maximum values at the milk-ripe stage. Final plant heights under B0, B1, B2, and B3 were 98, 101, 97, and 106 cm, respectively. Compared with B0, plant height increased by 3.06% under B1 and 8.16% under B3 but decreased by 1.02% under B2. B3 generally maintained greater plant height during the middle and late growth stages, particularly after 17 July, although differences among treatments narrowed after August.

Aboveground dry matter per hill remained relatively low during regreening and tillering, increased rapidly during jointing and booting, and continued to accumulate until the milk-ripe stage. At this stage, compared with B0, aboveground dry matter under B1 and B2 was 4.53% and 5.94% lower, respectively, whereas B3 showed a 14.04% increase. Leaf area generally increased during the early growth stages, reached its maximum at heading and flowering, and declined at the milk-ripe stage. At heading and flowering, B2

exhibited the largest leaf area (29.07 cm²), followed by B3 (28.57 cm²). Compared with B0, leaf area decreased by 3.64% under B1 but increased by 9.41% and 7.53% under B2 and B3, respectively. At the milk-ripe stage, leaf area under B1, B2, and B3 exceeded that under B0 by 20.20%, 33.45%, and 30.90%, respectively, with B2 and B3 maintaining relatively high values of 26.20 and 25.70 cm². Overall, B2 and B3 maintained greater leaf area during the middle and late growth stages, with their relative advantages becoming more pronounced at the milk-ripe stage.

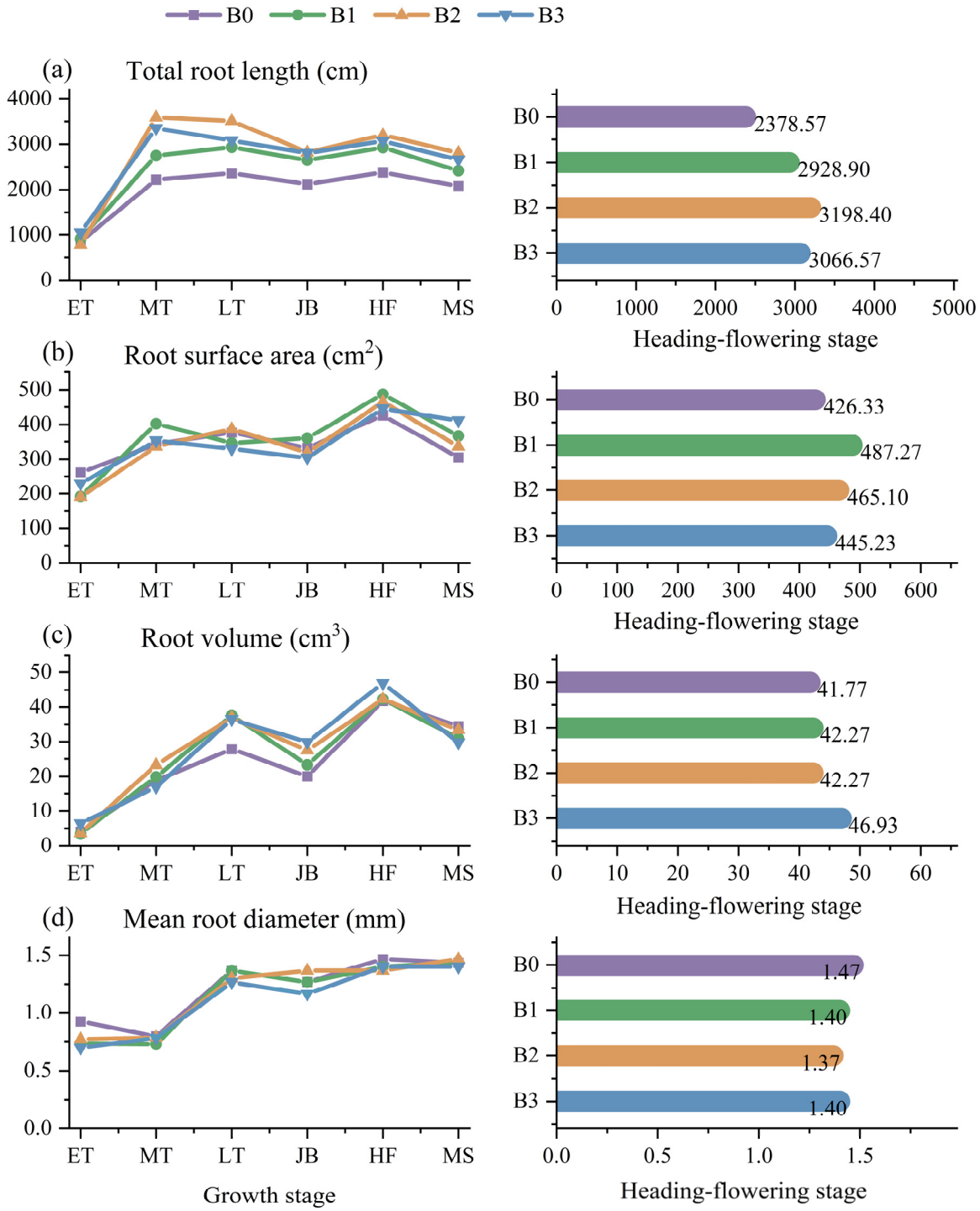


Figure 1. Changes in rice root morphological traits across growth stages and comparisons among treatments at the heading and flowering stage. (a) total root length; (b) root

volume; and (d) mean root diameter. Note: ET, MT, LT, JB, HF, and MS denote the early tillering, middle tillering, late tillering, jointing and booting, heading and flowering, and milk-ripe stages, respectively.

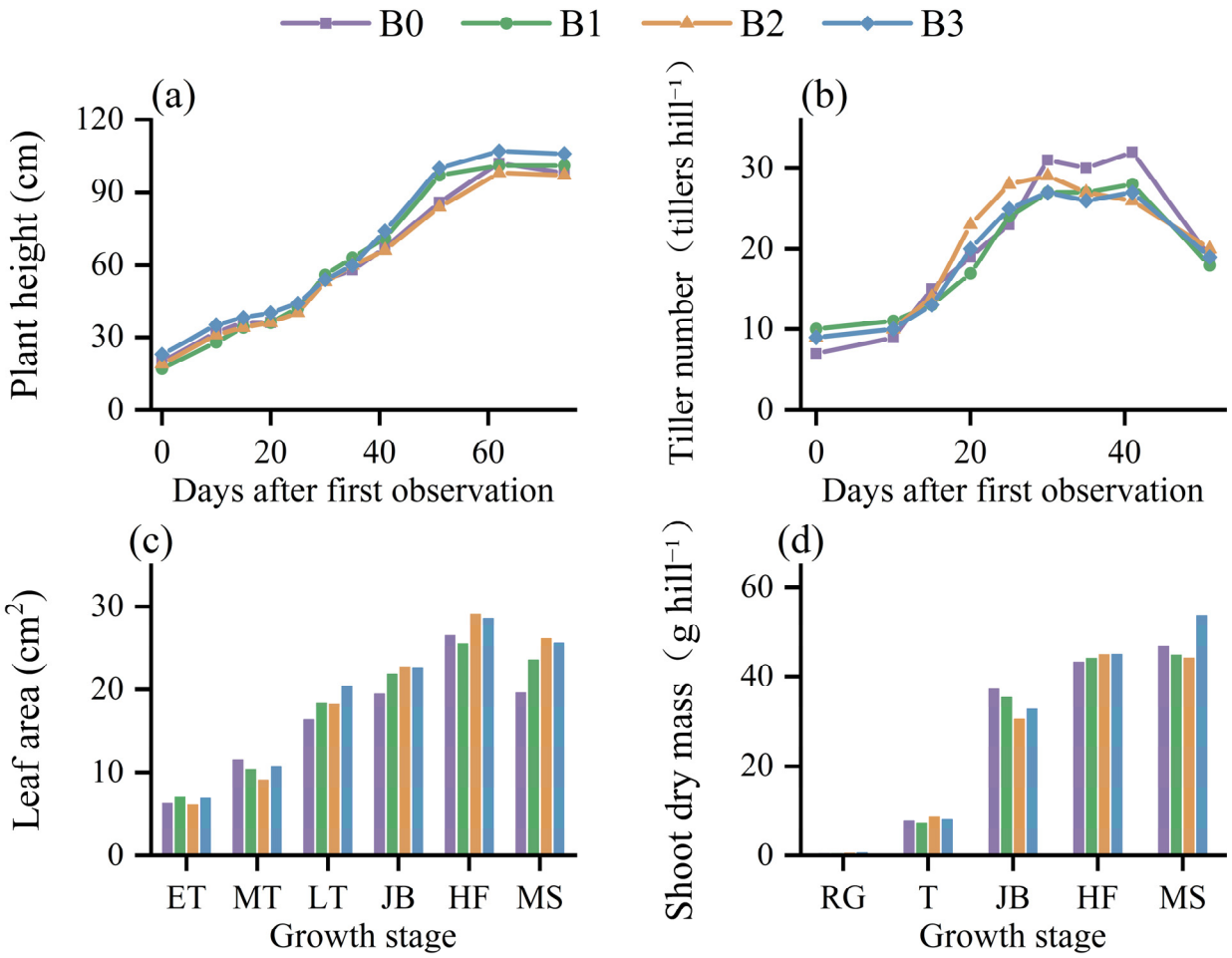


Figure 2. Changes in rice agronomic traits and aboveground dry matter accumulation across growth stages under different biochar application rates. (a) plant height; (b) tiller number; (c) leaf area; and (d) shoot dry mass.

As shown in Figure 3, rice yield components exhibited different responses to biochar application rates. Compared with B0, the number of effective panicles under B1, B2, and B3 increased by 3.03%, 9.09%, and 1.52%, respectively, with B2 showing the highest value (24.00 panicles per hill). The number of grains per panicle decreased by 4.91% and 0.54% under B1 and B2, respectively, but increased by 2.65% under B3, reaching 85.89 grains per panicle. The seed-setting rate under B1 was slightly lower than that under B0, whereas B2 and B3 showed increases of 0.62% and 1.37%, respectively, with B3 reaching the highest value of 98.02%. Thousand-grain weight increased by 4.35%, 0.32%, and 5.40% under B1, B2, and B3, respectively, with B3 reaching 26.01 g. Overall, B2 exhibited the greatest increase in effective panicle number, whereas B3 showed relatively higher values for grains per panicle, seed-setting rate, and thousand-grain weight, indicating that rice yield components responded differently to biochar application rates.

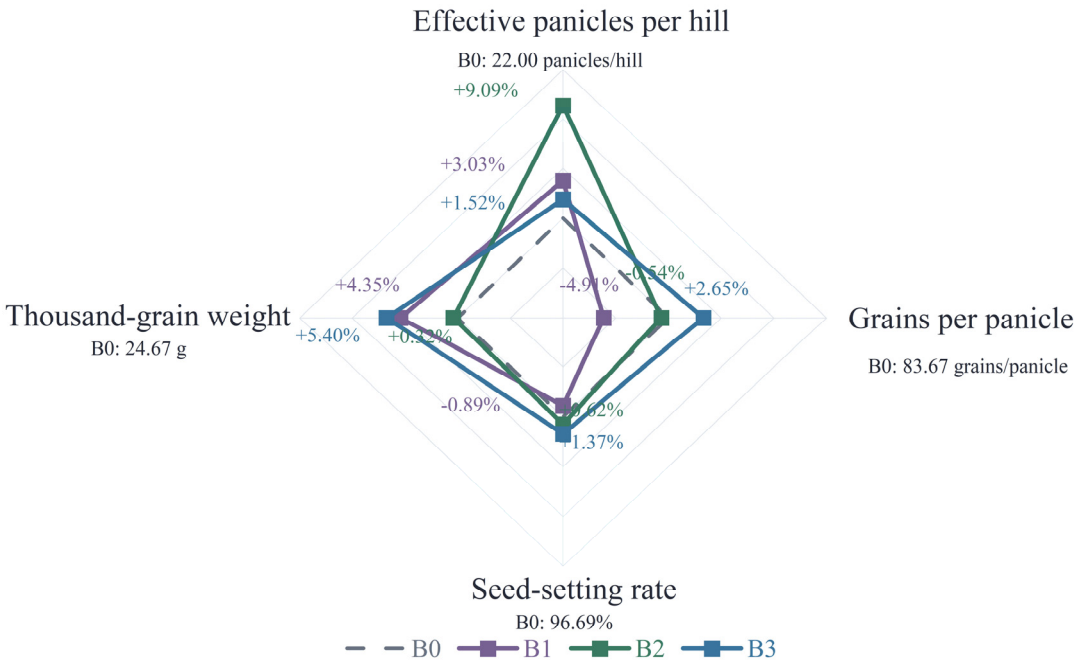


Figure 3. Relative changes in rice yield components under different biochar application rates.

3.3. Effects of Biochar Application Rates on Rice Photosynthetic Characteristics

Figure 4 illustrates the changes in net photosynthetic rate, stomatal conductance, transpiration rate, and intercellular CO_2 concentration across rice growth stages under different biochar treatments. The net photosynthetic rate initially increased and subsequently decreased during the growing season, reaching relatively high levels at the jointing and booting stage and remaining relatively stable at heading and flowering. At jointing and booting, B1 exhibited the highest net photosynthetic rate (15.05), whereas B2 showed the lowest value (14.50), with relatively small differences among treatments. At heading and flowering, compared with B0, net photosynthetic rates under B1, B2, and B3 were 3.10%, 2.37%, and 2.53% higher, respectively, although these differences were not significant ($p > 0.05$). At the milk-ripe stage, the corresponding increases were 7.72%, 4.05%, and 9.30%, with B3 and B1 maintaining relatively higher rates.

Stomatal conductance varied among treatments across growth stages. B0 generally exhibited higher values at late tillering and jointing and booting, whereas B1 showed relatively higher values at middle tillering. B3 exhibited a marked increase at heading and flowering, while B2 showed comparatively moderate fluctuations throughout the growing season. At heading and flowering, compared with B0, stomatal conductance under B1 and B2 was 15.99% and 62.45% lower, respectively, whereas B3 showed a 33.88% increase. However, none of these differences were significant ($p > 0.05$). Stomatal conductance values converged among treatments at the milk-ripe stage.

Transpiration rate also exhibited growth-stage-dependent variations. B3 generally maintained relatively high transpiration rates during the early and late growth stages, particularly from heading and flowering to the milk-ripe stage. B1 and B2 showed relatively rapid increases during middle tillering but declined below B0 at late tillering. At jointing and booting, compared with B0, transpiration rates under B1, B2, and B3 were 7.43%, 11.59%, and 10.90% lower, respectively. In contrast, B3 exhibited increases of 10.13% and 15.35% at heading and flowering and the milk-ripe stage, respectively.

Intercellular CO_2 concentration was relatively high before tillering, with B2 showing the highest value (335.30), followed by B1 (329.40), B3 (321.84), and B0 (319.00). B2

maintained relatively higher values during middle tillering and jointing and booting, while B1 and B3 showed higher values at late tillering and heading and flowering, respectively. At the milk-ripe stage, intercellular CO_2 concentrations under all three biochar treatments were higher than that under B0, although the differences among treatments were not significant.

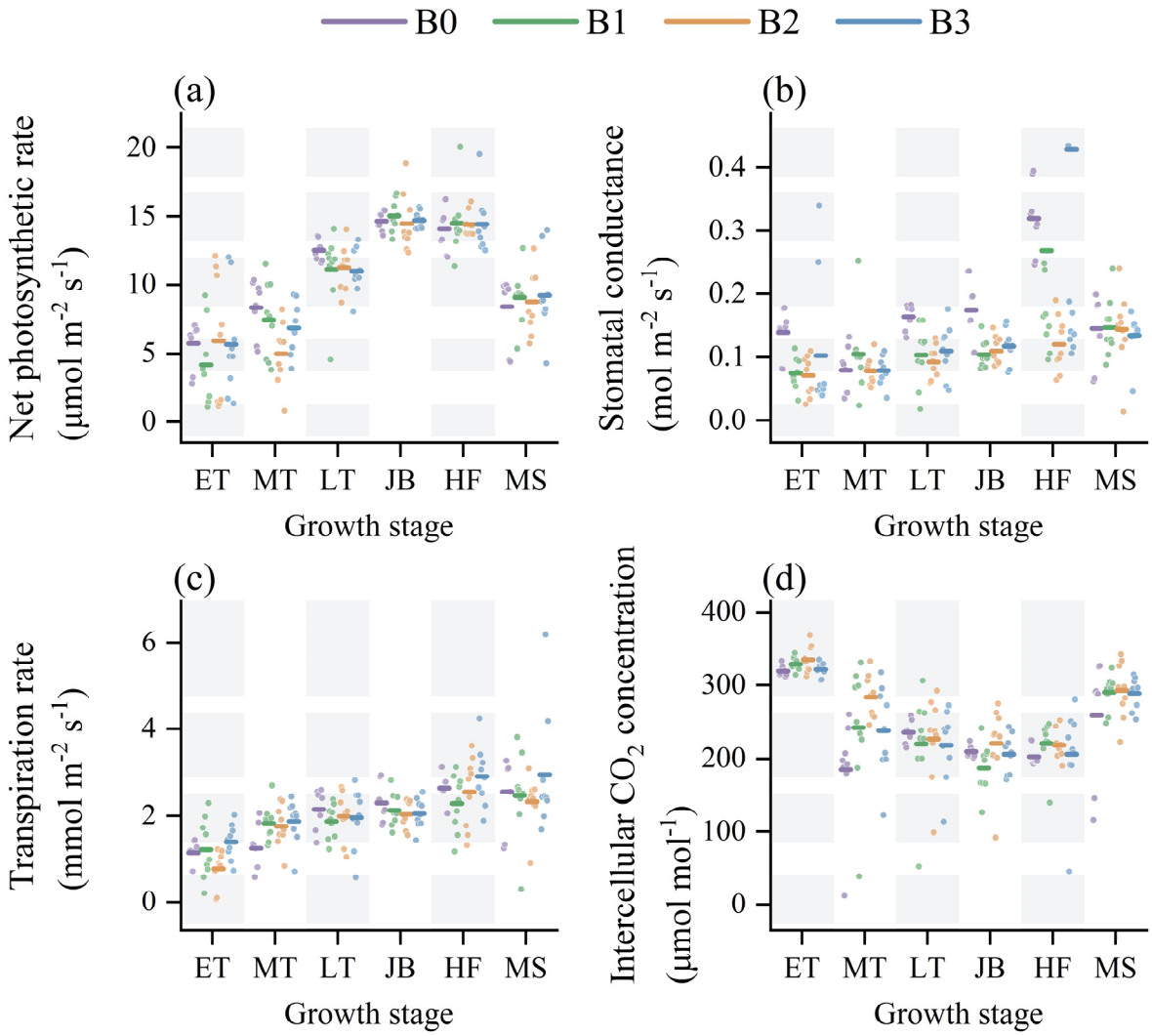


Figure 4. Changes in rice photosynthetic parameters across growth stages under different biochar application rates. (a) net photosynthetic rate; (b) stomatal conductance; (c) transpiration rate; and (d) intercellular CO_2 concentration.

3.4. Effects of Biochar Application Rates on Soil Water, Thermal, and Salinity Conditions at Different Depths in Paddy Fields

Soil temperature exhibited similar temporal patterns across biochar treatments, with pronounced fluctuations over time and clear vertical variations among soil depths (Figure 5). During the observation period, soil temperature fluctuated with ambient air temperature, increasing notably in early June, from late June to early July, and in mid-July, followed by subsequent declines. The surface (0 cm) and 10 cm soil layers were more responsive to ambient temperature changes and exhibited greater fluctuations. Temperature fluctuations gradually decreased with increasing soil depth, with the smallest variations observed at 40 cm, reflecting greater temperature stability in deeper soil layers.

Differences among biochar treatments were most apparent in the shallow soil layers. B1 exhibited relatively large temperature fluctuations at 0 cm from early June to mid-July, while B2 showed pronounced variations at 0 and 10 cm from late June to mid-July. Under B3, surface soil temperature increased markedly during the warming periods in late June and mid-July. Similarly, B0 exhibited substantial fluctuations in shallow soil temperature, with relatively high values recorded in late June, early July, and mid-July. As soil depth increased, temperature fluctuations and differences among treatments gradually diminished. The mean soil temperatures at depths of 0, 10, 20, 30, and 40 cm under B0 during the observation period were 21.06, 19.10, 17.35, 16.92, and 16.78 °C, respectively. Compared with B0, the mean temperatures at depths of 10–30 cm increased by 1.35–3.03 °C, 1.35–2.79 °C, and 2.02–3.43 °C under B1, B2, and B3, respectively. At a depth of 20 cm, the mean temperature under B3 was 3.43 °C higher than that under B0. At the soil surface (0 cm), differences in mean temperature among treatments were relatively small. At 40 cm, mean temperatures under B1 and B2 were lower than that under B0, whereas B3 showed a comparable value. Overall, the effects of biochar on soil temperature varied with soil depth and application rate, without a consistent increasing or decreasing trend as the application rate increased.

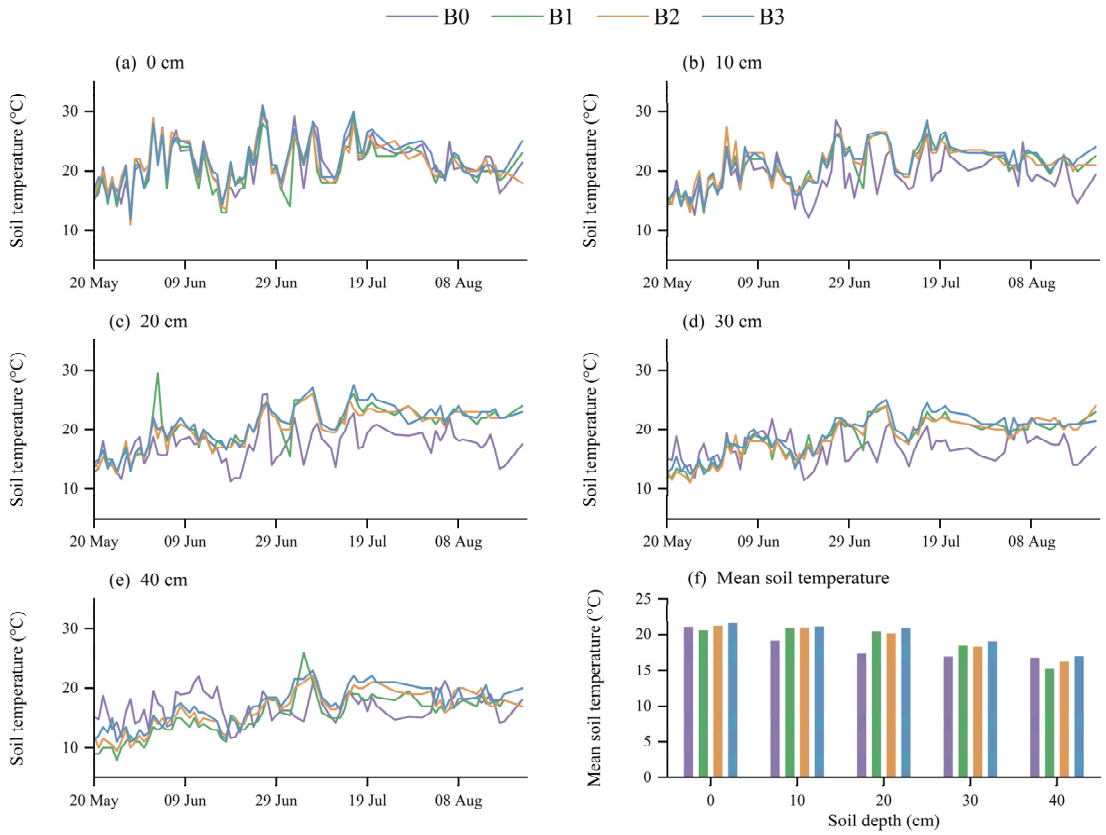


Figure 5. Temporal variations and mean values of soil temperature at different depths in paddy fields under different biochar application rates.

Soil salinity and moisture exhibited pronounced vertical variations across the soil profile under different biochar treatments (Figure 6). During the observation period, mean soil salinity generally decreased with increasing depth, with the highest values observed in the 0–20 cm layer. In this layer, B0 exhibited the highest salinity value (11.03), exceeding those under B1, B2, and B3. Although soil salinity generally declined with depth across treatments, differences in salinity distribution were observed in the middle and deeper

soil layers. Compared with B0, mean soil salinity under B1 decreased by 70.98%, 60.72%, 52.93%, 52.81%, and 59.78% in the 0–20, 20–40, 40–60, 60–80, and 80–100 cm layers, respectively. Under B2, the corresponding reductions in the upper four layers were 54.39%, 55.29%, 44.66%, and 41.54%, whereas salinity increased by 12.82% in the 80–100 cm layer. Under B3, mean soil salinity decreased by 45.76%, 67.64%, 61.80%, 31.76%, and 11.50% across the five soil layers, respectively. Overall, B1 showed relatively consistent reductions in salinity throughout the soil profile, while B3 exhibited greater reductions in the 20–60 cm layers. In contrast, B2 showed increased salinity in the deepest layer (80–100 cm). It should be noted that the above percentage changes in soil salinity were calculated by comparing the mean values of each biochar treatment with those of the control during the observation period. These values reflect relative differences in soil salinity profiles among treatments rather than actual changes in salt content within the same soil layer before and after biochar application.

Soil moisture content generally increased with depth, with higher values observed in deeper soil layers than in the surface layer. In the 0–20 cm layer, soil moisture content was relatively low across treatments, with B2 and B3 showing higher values, followed by B1 and B0. Soil moisture content gradually increased with depth under all treatments, and B2 and B3 maintained higher values than B1 and B0 in the 80–100 cm layer. Compared with B0, soil moisture content under B1 increased by 8.48%, 11.37%, and 3.61% in the 0–20, 20–40, and 40–60 cm layers, respectively, but decreased by 1.57% and 4.49% in the 60–80 and 80–100 cm layers, respectively. In contrast, B2 and B3 increased soil moisture content across all soil layers by 4.26–21.10% and 5.83–25.21%, respectively. Overall, B3 exhibited the greatest increase in soil moisture content, particularly in the 40–60 cm layer, followed by B2, whereas the positive effects of B1 were mainly concentrated in the upper 0–60 cm soil profile.

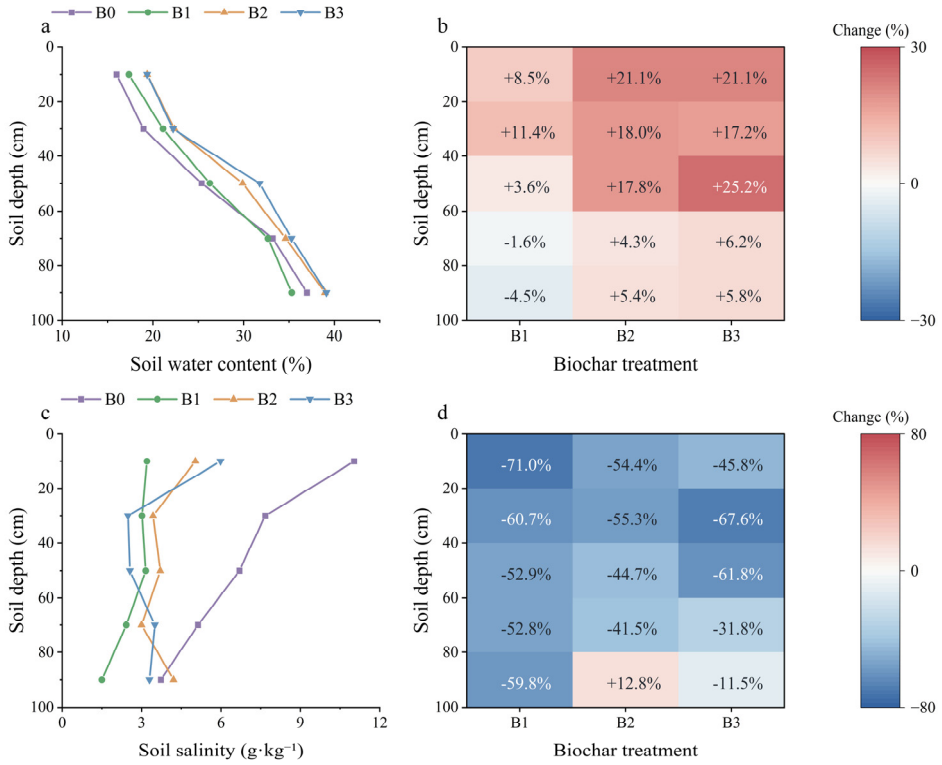


Figure 6. Soil water and salt profiles in paddy fields and their changes relative to the control under different biochar application rates. (a) soil water content profiles; (b) changes in soil water content relative to the control; (c) soil salinity profiles; and (d) changes in soil salinity relative to the control.

https://doi.org/10.3390/su182312168

3.5. Integrated Assessment of Different Biochar Treatments

The weights assigned to the evaluation indicators using the LOPCOW method are presented in Figure 7. Among the four categories, growth traits had the highest cumulative weight (30.05%), followed by photosynthetic traits (26.98%), root characteristics (25.55%), and soil moisture, temperature, and salinity indicators (17.43%). At the individual indicator level, net photosynthetic rate had the highest weight (9.12%), followed by soil salinity (8.97%) and total root length (8.90%). Intercellular CO_2 concentration, tiller number, and grain weight had similar weights of 7.45%, 7.44%, and 7.41%, respectively. Root volume had the lowest weight (2.91%), while soil temperature variability also received a relatively low weight (3.38%). Overall, the most heavily weighted individual indicators were associated with photosynthesis, soil salinity, and root development, whereas growth traits contributed the largest share of the total weight at the category level.

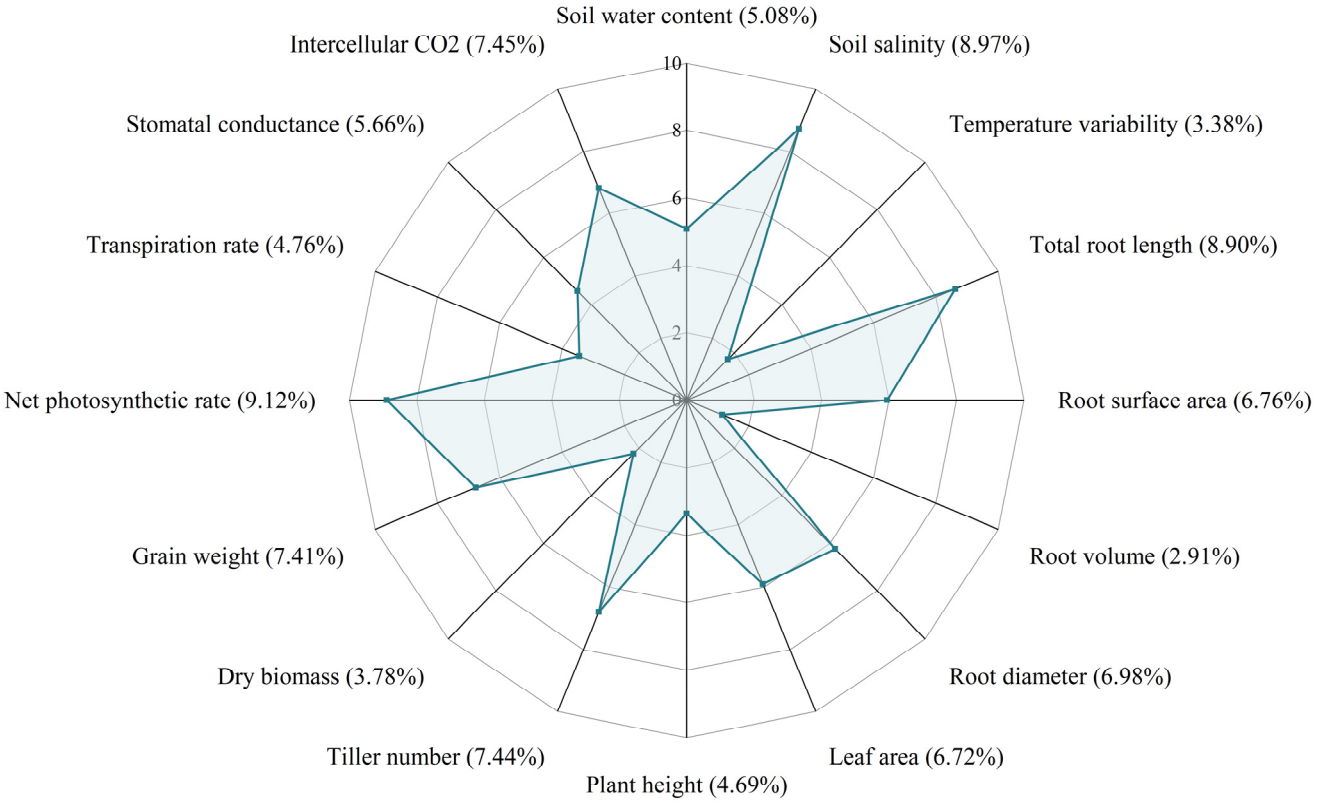


Figure 7. Indicator weights determined using the LOPCOW method for the integrated assessment of soil conditions and rice growth.

The SPOTIS evaluation results are presented in Figure 8. All three biochar treatments achieved higher overall scores than the control, with the treatments ranked in descending order as B3 > B2 > B1 > B0. B3 had the smallest overall distance (0.38) and the highest overall score (0.62), followed by B2 (distance: 0.40; score: 0.60) and B1 (distance: 0.44; score: 0.56). In contrast, B0 had the largest overall distance (0.81) and the lowest score (0.19). Within the biochar application range of 5–15 t ha^{-1}, the overall distance decreased and the overall score increased with increasing application rate. The score differences between the biochar treatments and the control were greater than those among the biochar treatments, with B3 and B2 showing particularly similar scores. Consistent with the individual indicator results, B2 performed relatively better in total root length, whereas B3 showed advantages in plant height during the later growth stages, aboveground dry matter at the milk-ripe stage, and grain weight. Considering soil conditions, root characteristics,

growth traits, and photosynthetic traits, the 15 t ha^{-1} treatment achieved the highest overall score, followed by 10 t ha^{-1}.

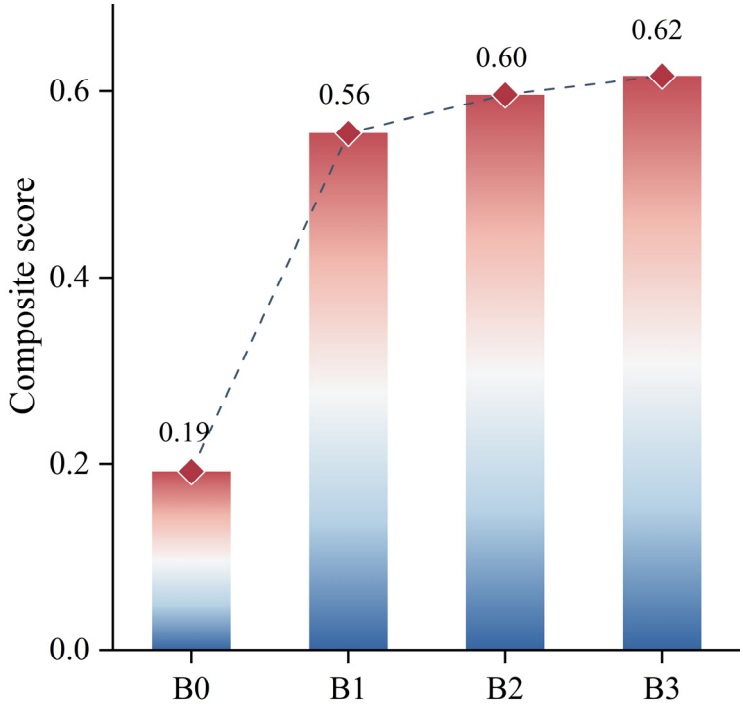


Figure 8. Overall scores of different biochar treatments determined using the SPOTIS method.

To assess the sensitivity of the overall evaluation results to indicator weighting and normalization methods, a sensitivity analysis was conducted under three alternative scenarios based on the original LOPCOW–SPOTIS evaluation. These scenarios included: (1) replacing the LOPCOW-derived weights with equal weights; (2) excluding four potentially debatable indicators (soil moisture content, mean root diameter, transpiration rate, and stomatal conductance) and renormalizing the weights of the remaining indicators; and (3) replacing the mean reference values of the five target-type indicators with median values, followed by recalculation of normalized indicator values and LOPCOW weights. The overall scores and rankings under different scenarios are presented in Table 2. The treatment ranking remained unchanged across all scenarios, following the order B3 > B2 > B1 > B0. Under the equal-weight scenario, B3 achieved the highest overall score (0.5909). After excluding the four indicators, B3 remained the highest-ranked treatment, with a score of 0.7087. Similarly, replacing the mean reference values with median values yielded a score of 0.6466 for B3 without altering the treatment ranking. Although the overall scores varied across evaluation scenarios, the consistent ranking indicates that the evaluation results exhibited a degree of robustness to changes in indicator weights and normalization reference values.

Table 2. Overall scores and rankings of different biochar treatments under different evaluation scenarios.

Evaluation Scenario	B0	B1	B2	B3	Ranking
LOPCOW–SPOTIS	0.1923	0.5550	0.5962	0.6163	B3 > B2 > B1 > B0
Equal weighting	0.2405	0.4755	0.5178	0.5909	B3 > B2 > B1 > B0
Exclusion of four indicators	0.1370	0.5540	0.6722	0.7087	B3 > B2 > B1 > B0
Median-based normalization	0.1984	0.5860	0.6105	0.6466	B3 > B2 > B1 > B0

4. Discussion

4.1. Effects of Biochar on the Distribution of Soil Water, Heat, and Salts in Paddy Fields

In this study, the effects of biochar on soil moisture and salinity did not improve consistently with increasing application rate. Soil moisture content under B2 and B3 was generally higher than that under the control across all soil layers, whereas the moisture-enhancing effect of B1 was mainly confined to the upper soil layers, indicating application-rate-dependent differences in soil moisture distribution. The internal pore structure of biochar and its influence on soil particle arrangement can modify soil water storage and transport, although these effects depend on soil texture, biochar properties, and application rate [33–36]. Therefore, the higher soil moisture content observed under B2 and B3 may be associated with improved soil water retention. However, soil moisture content reflects the water status at the time of measurement and does not necessarily indicate increased plant-available water or enhanced infiltration capacity. Regarding soil salinity, the effects of biochar varied considerably with application rate and soil depth. Mean soil salinity under B1 was lower than that under B0 across all soil layers, with reductions of 52.81–70.98%. Under B2, mean salinity decreased by 41.54–55.29% in the 0–80 cm layers but increased by 12.82% in the 80–100 cm layer. B3 also exhibited lower salinity across all soil layers, although the reductions varied with depth. These findings indicate that biochar effects on soil salinity distribution were dependent on both application rate and soil depth, rather than increasing consistently with application rate. The porous structure of biochar may alter soil pore distribution and water transport conditions, thereby influencing irrigation water infiltration and vertical salt transport. Previous studies have shown that biochar can affect salt leaching by modifying soil porosity and saturated hydraulic conductivity, although these effects depend on soil properties and application conditions [37,38]. Moreover, biochar surface properties and soluble constituents may influence soil salinity distribution through ion adsorption and exchange processes [39].

Biochar may therefore influence soil salinity profiles by modifying soil water transport conditions and ion exchange processes. The higher salinity observed in the 80–100 cm layer under B2 suggests possible vertical salt redistribution, although the direction of salt transport and dominant mechanisms remain uncertain. Salt transport is also influenced by irrigation, drainage, evaporation, and soil moisture gradients. However, the lack of initial soil salinity profiles and systematic monitoring of irrigation and drainage volumes and their salt concentrations prevented the establishment of a complete soil water and salt balance. Consequently, the relative contributions of salt leaching and internal redistribution could not be reliably distinguished, nor could the net salt removal from the entire soil profile be determined. Thus, the present results primarily reflect differences in soil salinity distribution among treatments during the observation period, and the underlying mechanisms require further investigation.

Soil temperature exhibited greater fluctuations in the shallow layers and more gradual variations in deeper layers, with differences among treatments diminishing with increasing soil depth. This pattern is consistent with the direct influence of solar radiation, air temperature, and irrigation on surface soil, whereas temperature fluctuations in deeper layers are attenuated and delayed. Biochar can modify soil thermal conductivity, heat capacity, and surface albedo; however, the resulting temperature responses also depend on soil moisture conditions and surface cover, and changes in thermal properties do not necessarily produce consistent warming or cooling effects [40]. Moreover, soil moisture and heat transfer are closely coupled, as variations in soil moisture content can affect soil heat capacity and thermal conductivity, thereby altering heat storage and transfer. Thus, differences in soil moisture content among biochar treatments may partly contribute to the observed variations in soil temperature across depths. During the observation period,

mean soil temperatures under biochar treatments were generally higher than those under the control at depths of 10–30 cm, whereas the responses at 0 and 40 cm were inconsistent. These findings indicate that the effects of biochar on soil temperature varied with depth, without a consistent overall warming or thermal buffering effect. Importantly, soil temperature monitoring was primarily conducted during the rice growing season and did not cover winter freezing or spring thawing. Therefore, the results characterize temperature variations only during the observation period and cannot establish the effects of biochar on soil freezing, thawing, or freeze–thaw cycles, nor do they provide sufficient evidence of its potential thermal insulation effects during winter.

4.2. Effects of Biochar on Rice Root and Shoot Growth

At the heading and flowering stage, total root length was higher under all biochar treatments than under the control, with the greatest increase observed in B2. The largest increases in root surface area and root volume were observed under B1 and B3, respectively, indicating that different biochar application rates had varying effects on rice root morphological traits. A previous meta-analysis has shown that the effects of biochar on root length, diameter, and biomass differ in magnitude and are influenced by soil conditions and biochar properties [41]. These morphological responses may be associated with improvements in soil physical conditions, as well as the nutrient content of biochar and its effects on rhizosphere nutrient availability [42,43]. Evidence from wheat experiments further suggests that biochar-induced changes in nutrient availability may partly explain variations in root development, highlighting the importance of considering nutrient availability when interpreting root morphological responses [44]. Considering the observed changes in soil moisture and salinity, the higher soil moisture content under B2 and B3 may have provided more favorable moisture conditions for root growth. However, the higher salinity observed in the 80–100 cm layer under B2 indicates that increased soil moisture does not necessarily correspond to reduced salinity throughout the soil profile. The vertical distributions of soil moisture and salinity may jointly influence the root-zone environment and be associated with aboveground rice growth, although the underlying mechanisms remain unclear.

In this study, B2 exhibited the greatest increase in total root length, yet its aboveground dry biomass at the milk-ripe stage remained lower than that of the control. In contrast, although B3 did not show the greatest increase in total root length, its aboveground dry biomass was 14.04% higher than that of the control. This contrast suggests that greater root development does not necessarily correspond to increased aboveground biomass accumulation. Root growth is also influenced by biochar application rate, plant species, and soil nutrient conditions, and greater root development does not necessarily lead to improvements in all growth traits [45]. Furthermore, the relatively higher soil moisture content, leaf area, and net photosynthetic rate under B3 during the later growth stages were consistent with its greater dry matter accumulation, suggesting that these factors may have jointly favored biomass accumulation. However, their individual contributions remain to be determined. The absence of significant differences in tiller number further indicates that rice growth responses varied among traits and that the beneficial effects of biochar were not evident across all growth indicators.

4.3. Effects of Biochar on Rice Photosynthetic Characteristics

The effects of biochar on net photosynthetic rate varied across rice growth stages. At heading and flowering, net photosynthetic rates under all biochar treatments were slightly higher than that under the control, although the differences were not significant. At the milk-ripe stage, B1 and B3 maintained relatively higher rates, indicating more pronounced treatment differences during the later growth stages. A previous meta-analysis

has shown that biochar effects on photosynthetic rate depend on soil properties, biochar characteristics, and fertilizer inputs, with considerable variability across experimental conditions [46]. A broader synthesis of plants with different photosynthetic pathways also revealed variable responses in photosynthetic rate, stomatal conductance, and transpiration rate, suggesting that overall average effects cannot be directly applied to individual field treatments [47]. In this study, the relatively higher net photosynthetic rate and leaf area under B3 during the later growth stages were consistent with its greater aboveground dry matter accumulation. However, instantaneous leaf-level measurements cannot fully represent canopy-level or season-long carbon assimilation.

Stomatal conductance, transpiration rate, and intercellular CO_2 concentration did not change consistently with net photosynthetic rate, indicating that differences in leaf gas exchange among treatments cannot be fully explained by a single parameter. Increased intercellular CO_2 concentration may reflect changes in stomatal diffusion or leaf carbon assimilation capacity rather than necessarily indicating enhanced photosynthesis. Similarly, higher transpiration rates do not necessarily imply improved water use efficiency. An isotope-tracing study in rice showed that biochar application could increase photosynthetic carbon accumulation in the plant–soil system without significantly altering its allocation proportions, highlighting the distinction between total carbon assimilation and carbon allocation patterns [48]. In the present study, the responses of root morphology, leaf physiological parameters, and dry matter accumulation were not fully synchronized, suggesting that individual root or photosynthetic indicators alone cannot adequately explain variations in rice biomass accumulation.

4.4. Integrated Assessment and a Suitable Biochar Application Rate

The overall evaluation ranked the treatments in descending order as B3 > B2 > B1 > B0. B1 showed relatively consistent reductions in salinity throughout the soil profile, B2 exhibited an advantage in total root length, and B3 showed higher soil moisture content and greater dry matter accumulation during the later growth stages. These findings indicate that advantages in individual indicators do not necessarily correspond to overall performance, highlighting the need to consider both soil conditions and crop growth when selecting an appropriate biochar application rate. The 15 t ha^{-1} treatment achieved the highest overall score, although the difference from the 10 t ha^{-1} treatment was relatively small, indicating that both application rates performed well within the evaluation framework used in this study. However, the effectiveness of biochar under field conditions depends not only on application rate but also on biochar quality, initial soil conditions, climatic conditions, and field management practices. Previous studies have demonstrated the potential of biochar to improve soil conditions and enhance agricultural productivity, although its effectiveness depends on biochar quality and application conditions [49]. Furthermore, the effects of biochar may evolve over time due to dissolution, surface reactions, and aging processes after soil incorporation. Therefore, evaluation results from a single growing season may not adequately reflect its long-term performance [50]. Furthermore, higher biochar application rates generally require greater material inputs, and their practical value should be evaluated by considering the costs of biochar procurement, transportation, and field application. Previous studies have shown that biochar effects on crop yield vary with fertilizer co-application and application duration [51]. However, this study did not assess biochar application costs, and the limited observation period prevented an evaluation of the long-term effects of biochar application on soil productivity and its stability. Furthermore, the overall evaluation results were influenced by indicator orientations, weighting schemes, and normalization methods. For target-type indicators, the mean value across treatments was used as the normalization reference point solely for relative comparisons among treatments, rather than as a validated physiological optimum.

In addition, yield components, including effective panicle number, grains per panicle, seed-setting rate, and thousand-grain weight, were measured in this study. The results showed that different biochar application rates had varying effects on traits associated with rice yield formation. However, reliable final grain yield data were unavailable, making it difficult to determine the effects of different treatments on actual rice yield. Therefore, the integrated assessment primarily reflects the relative performance of the treatments based on the measured indicators, and the effects of biochar application on final rice grain yield require further investigation. Although the 15 t ha^{-1} treatment showed favorable overall performance under the experimental conditions, its practical suitability requires further validation considering biochar application costs, initial soil conditions, and results from multi-year field trials. From the perspective of sustainable rice production in cold regions, biochar application should balance soil water retention, salinity distribution across the soil profile, and rice growth responses rather than rely on a single soil or crop indicator. The distinct responses to different application rates in terms of soil moisture, salinity, root development, and aboveground dry matter accumulation highlight the multifaceted and condition-dependent effects of biochar. Accordingly, selecting an appropriate application rate requires an integrated consideration of initial soil conditions, irrigation and drainage management, biochar input costs, and crop growth requirements.

This study has several limitations. First, the field experiment was conducted at a single site in Qing'an County, Heilongjiang Province, China, which may limit the applicability of the findings to other regions and soil conditions. Second, although the experimental period covered a complete seasonal freeze–thaw cycle, soil temperature monitoring was primarily conducted during the rice growing season, without continuous measurements during winter freezing and spring thawing. Consequently, the effects of biochar on soil freeze–thaw processes and thermal conditions in cold-region paddy fields could not be fully evaluated. In addition, although yield components, including effective panicle number, grains per panicle, seed-setting rate, and thousand-grain weight, were measured, reliable final grain yield data were unavailable, limiting the assessment of biochar effects on actual rice yield. Furthermore, the lack of multi-year field observations and economic analysis prevented a comprehensive evaluation of the long-term effects of different biochar application rates on soil improvement, agricultural productivity, and economic feasibility. Therefore, the 15 t ha^{-1} treatment can currently be regarded as a relatively favorable option under the experimental conditions of this study, but its practical suitability requires further validation. Future research should involve multi-site, multi-year field experiments under different soil conditions, incorporate continuous soil temperature monitoring during winter freezing and spring thawing, improve the measurement of final rice grain yield, and include cost–benefit analysis. These efforts would provide a stronger basis for understanding the long-term effects of biochar application on soil moisture, temperature, salinity, and rice productivity in cold-region paddy fields and for determining appropriate biochar application rates.

5. Conclusions

This study investigated the effects of different biochar application rates on soil moisture, temperature, salinity distribution, and rice growth in a cold-region paddy field and evaluated treatment performance using the LOPCOW–SPOTIS method. The main conclusions are as follows:

(1) The effects of biochar on soil moisture and salinity varied with application rate and soil depth, and improvements in soil moisture and reductions in salinity did not increase consistently with increasing application rates. Based on mean values over the observation period, soil moisture content at all monitored depths was 4.26–21.10% and 5.83–25.21% higher than the control under the 10 and 15 t ha^{-1} treatments, respectively. The

increase in soil moisture under the 5 t ha^{-1} treatment was mainly confined to the 0–60 cm soil layer. Mean soil salinity was lower than the control at all monitored depths under the 5 and 15 t ha^{-1} treatments, with the 5 t ha^{-1} treatment showing a more consistent reduction across the soil profile. In contrast, the 10 t ha^{-1} treatment reduced mean soil salinity at depths of 0–80 cm but increased it at 80–100 cm. Soil temperature fluctuations decreased with increasing depth during the observation period, with differences among treatments occurring primarily in the upper soil layers.

(2) Biochar application had differing effects on rice root morphology and aboveground growth. At the heading and flowering stage, total root length was greater under all biochar treatments than under the control, with the largest increase (34.47%) observed at 10 t ha^{-1}. The 5 and 15 t ha^{-1} treatments showed relatively large increases in root surface area and root volume, respectively. At the milk-ripe stage, aboveground dry biomass was 14.04% higher than the control under the 15 t ha^{-1} treatment but 4.53% and 5.94% lower under the 5 and 10 t ha^{-1} treatments, respectively. Mean leaf area and net photosynthetic rate at the milk-ripe stage were generally higher under biochar treatments than under the control. However, differences among treatments in net photosynthetic rate at the heading and flowering stage and in tiller number across growth stages were not statistically significant.

(3) The advantages of individual indicators did not fully correspond to the overall treatment performance. The LOPCOW–SPOTIS evaluation showed that all three biochar treatments achieved higher overall scores than the control, with the 15 t ha^{-1} treatment ranking first, followed by the 10 t ha^{-1} treatment. Considering soil moisture, temperature, salinity, and rice growth responses, the 15 t ha^{-1} treatment showed the best overall performance under the experimental conditions and evaluation framework of this study. These findings provide a reference for selecting appropriate biochar application rates in cold-region paddy fields under comparable soil and management conditions. However, the practical suitability of this application rate requires further validation through assessments of biochar application costs, baseline soil conditions, and multi-year field trials.

Author Contributions: X.H.: Project administration, Methodology, Investigation, Data curation. Z.F. and H.T.: Project administration, Methodology, Investigation, Data curation. E.Z.: Writing—review & editing, Funding acquisition, Conceptualization, Project administration. Z.Q.: Investigation, Formal analysis, Data curation. All authors have read and agreed to the published version of the manuscript.

Funding: Heilongjiang Provincial Natural Science Foundation Project (PL2025E071).

Institutional Review Board Statement: Not applicable.

Informed Consent Statement: Not applicable.

Data Availability Statement: The raw data supporting the conclusions of this article will be made available by the authors on request.

Acknowledgments: We are grateful for the support of all the authors.

Conflicts of Interest: Author HuiLing Tong was employed by the company Hangzhou Hydropower Construction Group Co., Ltd. The remaining authors declare that the research was conducted in the absence of any commercial or financial relationships that could be construed as a potential conflict of interest.

References

1. Lee, X.; Yang, F.; Xing, Y.; Huang, Y.; Xu, L.; Liu, Z.; Holtzman, R.; Kan, I.; Li, Y.; Zhang, L.; et al. Use of Biochar to Manage Soil Salts and Water: Effects and Mechanisms. *CATENA* **2022**, *211*, 106018. https://doi.org/10.1016/j.catena.2022.106018.
2. Munns, R.; Tester, M. Mechanisms of Salinity Tolerance. *Annu. Rev. Plant Biol.* **2008**, *59*, 651–681. https://doi.org/10.1146/annurev.arplant.59.032607.092911.
3. Gao, Y.; Li, T.; Fu, Q.; Li, H.; Liu, D.; Ji, Y.; Li, Q.; Cai, Y. Biochar Application for the Improvement of Water-Soil Environments and Carbon Emissions under Freeze-Thaw Conditions: An in-Situ Field Trial. *Sci. Total Environ.* **2020**, *723*, 138007. https://doi.org/10.1016/j.scitotenv.2020.138007.
4. Fu, Q.; Zhao, H.; Li, T.; Hou, R.; Liu, D.; Ji, Y.; Zhou, Z.; Yang, L. Effects of Biochar Addition on Soil Hydraulic Properties before and after Freezing-Thawing. *CATENA* **2019**, *176*, 112–124. https://doi.org/10.1016/j.catena.2019.01.008.
5. Lu, J.; Fu, H.; Wang, D.; Gao, J.; Li, H.; Chen, X. Temperature, Moisture, and Deformation Characteristics of Biochar-Stabilized Silty Clay during Freeze–Thaw Cycles. *J. Cold Reg. Eng.* **2026**, *40*, 04025052. https://doi.org/10.1061/JCRGEI.CRENG-1044.
6. Razzaghi, F.; Obour, P.B.; Arthur, E. Does Biochar Improve Soil Water Retention? A Systematic Review and Meta-Analysis. *Geoderma* **2020**, *361*, 114055. https://doi.org/10.1016/j.geoderma.2019.114055.
7. Yi, S.; Chang, N.Y.; Imhoff, P.T. Predicting Water Retention of Biochar-Amended Soil from Independent Measurements of Biochar and Soil Properties. *Adv. Water Resour.* **2020**, *142*, 103638. https://doi.org/10.1016/j.advwatres.2020.103638.
8. Alkhasha, A.; Al-Omran, A.; Alghamdi, A.G. Effect of Water Quality and Date Palm Biochar on Evaporation and Specific Hydrological Characteristics of Sandy Soil. *Agriculture* **2020**, *10*, 300. https://doi.org/10.3390/agriculture10070300.
9. Esmaeilnezhad, R.; Zeinalzadeh, K.; Besharat, S.; Kheirfam, H. Field Study on the Hydraulic Behavior of Heavy Soil: Effects of Biochar Application Rates. *Sci. Total Environ.* **2025**, *1004*, 180752. https://doi.org/10.1016/j.scitotenv.2025.180752.
10. Zhao, J.; Ren, T.; Zhang, Q.; Du, Z.; Wang, Y. Effects of Biochar Amendment on Soil Thermal Properties in the North China Plain. *Soil. Sci. Soc. Am. J.* **2016**, *80*, 1157–1166. https://doi.org/10.2136/sssaj2016.01.0020.
11. Chaganti, V.N.; Crohn, D.M.; Šimůnek, J. Leaching and Reclamation of a Biochar and Compost Amended Saline–Sodic Soil with Moderate SAR Reclaimed Water. *Agric. Water Manag.* **2015**, *158*, 255–265. https://doi.org/10.1016/j.agwat.2015.05.016.
12. Xu, Q.; Liu, H.; Li, M.; Li, P. The Presence of the Biochar Interlayer Effectively Inhibits Soil Water Evaporation and Salt Migration to the Soil Surface. *Agriculture* **2023**, *13*, 638. https://doi.org/10.3390/agriculture13030638.
13. Wang, X.; Ding, J.; Han, L.; Tan, J.; Ge, X.; Nan, Q. Biochar Addition Reduces Salinity in Salt-Affected Soils with No Impact on Soil pH: A Meta-Analysis. *Geoderma* **2024**, *443*, 116845. https://doi.org/10.1016/j.geoderma.2024.116845.
14. Su, Z.; Liu, X.; Wang, Z.; Wang, J. Biochar Effects on Salt-Affected Soil Properties and Plant Productivity: A Global Meta-Analysis. *J. Environ. Manag.* **2024**, *366*, 121653. https://doi.org/10.1016/j.jenvman.2024.121653.
15. Liu, B.; Li, H.; Li, H.; Zhang, A.; Rengel, Z. Long-term Biochar Application Promotes Rice Productivity by Regulating Root Dynamic Development and Reducing Nitrogen Leaching. *GCB Bioenergy* **2021**, *13*, 257–268. https://doi.org/10.1111/gcbb.12766.
16. Che, W.; Li, X.; Piao, J.; Zhang, Y.; Miao, S.; Wang, H.; Xie, L.; Jin, F. Biochar Improves Yield by Reducing Saline–Alkaline Stress, Enhancing Filling Rate of Rice in Soda Saline–Alkaline Paddy Fields. *Plants* **2024**, *13*, 2237. https://doi.org/10.3390/plants13162237.
17. Liu, Y.; Li, H.; Hu, T.; Mahmoud, A.; Li, J.; Zhu, R.; Jiao, X.; Jing, P. A Quantitative Review of the Effects of Biochar Application on Rice Yield and Nitrogen Use Efficiency in Paddy Fields: A Meta-Analysis. *Sci. Total Environ.* **2022**, *830*, 154792. https://doi.org/10.1016/j.scitotenv.2022.154792.
18. He, Y.; Chen, X.; Peng, Y.; Luo, Z.-B.; Jiang, S.-F.; Jiang, H. Investigation of the Effects of Biochar Amendment on Soil under Freeze–thaw Cycles and the Underlying Mechanism. *Heliyon* **2024**, *10*, e34907. https://doi.org/10.1016/j.heliyon.2024.e34907.
19. Acharya, B.S.; Dodla, S.; Wang, J.J.; Pavuluri, K.; Darapuneni, M.; Dattamudi, S.; Maharjan, B.; Kharel, G. Biochar Impacts on Soil Water Dynamics: Knowns, Unknowns, and Research Directions. *Biochar* **2024**, *6*, 34. https://doi.org/10.1007/s42773-024-00323-4.
20. Xu, Q.; Xu, Y.; Xia, H.; Han, H.; Li, M.; Gong, P.; Wang, C.; Li, Y.; Li, P.; Liu, H. Mitigation of Soil Salinity by Biochar and Halophytes. *Geoderma* **2025**, *454*, 117191. https://doi.org/10.1016/j.geoderma.2025.117191.
21. Pia, H.I.; Baek, N.; Park, S.-W.; Shin, E.-S.; Lee, S.-I.; Kim, H.-Y.; Tang, S.; Cheng, W.; Kwak, J.-H.; Park, H.-J.; et al. Luxury Application of Biochar Does Not Enhance Rice Yield and Methane Mitigation: A Review and Data Analysis. *J. Soils Sediments* **2024**, *24*, 2652–2668. https://doi.org/10.1007/s11368-024-03830-w.
22. Zhang, Z.; Zhang, Z.; Gong, Z.; Li, T.; Nie, T.; Chen, P.; Han, Y.; Xue, L. Biochar Application Combined with Water-Saving Irrigation Enhances Rice Root Growth and Nitrogen Utilization in Paddy Fields. *Agronomy* **2024**, *14*, 889. https://doi.org/10.3390/agronomy14050889.

23. Qin, X.; Li, Y.; Wang, H.; Liu, C.; Li, J.; Wan, Y.; Gao, Q.; Fan, F.; Liao, Y. Long-Term Effect of Biochar Application on Yield-Scaled Greenhouse Gas Emissions in a Rice Paddy Cropping System: A Four-Year Case Study in South China. *Sci. Total Environ.* **2016**, *569–570*, 1390–1401. https://doi.org/10.1016/j.scitotenv.2016.06.222.
24. Song Effects of Spring Irrigation Quotas on Water and Salt Distribution in Farmland with Different Degrees of Salinity and Alkalinity. *Water Sav. Irrig.* **2024**(4), 19–26. https://doi.org/10.12396/jsgg.2023452.
25. Sandhu, N.; Subedi, S.R.; Yadaw, R.B.; Chaudhary, B.; Prasai, H.; Iftekharuddaula, K.; Thanak, T.; Thun, V.; Battan, K.R.; Ram, M.; et al. Root Traits Enhancing Rice Grain Yield under Alternate Wetting and Drying Condition. *Front. Plant Sci.* **2017**, *8*, 1879. https://doi.org/10.3389/fpls.2017.01879.
26. Vishwakarma, C.; Krishna, G.K.; Kapoor, R.T.; Mathur, K.; Dalal, M.; Singh, N.K.; Mohapatra, T.; Chinnusamy, V. Physiological Analysis of Source–Sink Relationship in Rice Genotypes with Contrasting Grain Yields. *Plants* **2023**, *13*, 62. https://doi.org/10.3390/plants13010062.
27. Ecer, F.; Pamucar, D. A Novel LOPCOW-DOBI Multi-criteria Sustainability Performance Assessment Methodology: An Application in Developing Country Banking Sector. *Omega* **2022**, *112*, 102690. https://doi.org/10.1016/j.omega.2022.102690.
28. Dezert, J.; Tchamova, A.; Han, D.; Tacnet, J.-M. The SPOTIS Rank Reversal Free Method for Multi-Criteria Decision-Making Support. In *Proceedings of the 2020 IEEE 23rd International Conference on Information Fusion (FUSION)*; IEEE: Rustenburg, South Africa, 2020; pp. 1–8.
29. Aytekin, A. Comparative Analysis of the Normalization Techniques in the Context of MCDM Problems. *Decis. Mak. Appl. Manag. Eng.* **2021**, *4*, 1–25. https://doi.org/10.31181/dmame210402001a.
30. Yu, Y.; Zhu, J.; Guo, H. Research on the Measurement of Urban Economic Development Status in the Context of New Strategies—An Empirical Analysis Based on Social Network. *Stat. Res.* **2021**, *38*, 30–43. https://doi.org/10.19343/j.cnki.11-1302/c.2021.03.003.
31. Dua, T.V.; Duc, D.V.; Bao, N.C.; Trung, D.D. Integration of Objective Weighting Methods for Criteria and MCDM Methods: Application in Material Selection. *Eureka PE* **2024**, *2*, 131–148. https://doi.org/10.21303/2461-4262.2024.003171.
32. Kizielewicz, B.; Więckowski, J.; Shekhovtsov, A.; Wątróbski, J.; Depczyński, R.; Sałabun, W. Study towards the time-based MCDA ranking analysis—A supplier selection case study. *FU Mech. Eng.* **2021**, *19*, 381. https://doi.org/10.22190/FUME210130048K.
33. Edeh, I.G.; Mašek, O.; Buss, W. A Meta-Analysis on Biochar's Effects on Soil Water Properties—New Insights and Future Research Challenges. *Sci. Total Environ.* **2020**, *714*, 136857. https://doi.org/10.1016/j.scitotenv.2020.136857.
34. Omondi, M.O.; Xia, X.; Nahayo, A.; Liu, X.; Korai, P.K.; Pan, G. Quantification of Biochar Effects on Soil Hydrological Properties Using Meta-Analysis of Literature Data. *Geoderma* **2016**, *274*, 28–34. https://doi.org/10.1016/j.geoderma.2016.03.029.
35. Hu, J.; Yang, S.; Cornelis, W.M.; Huang, Q.; Qi, S.; Jiang, Z.; Qiu, H.; Xu, Y. Biochar Amendment Mitigates Negative Effects of Controlled Irrigation on Paddy Soil Structure: Insights from Micro-Pore Network Analysis. *Agric. Water Manag.* **2025**, *314*, 109517. https://doi.org/10.1016/j.agwat.2025.109517.
36. Jiang, Z.; Huang, S.; Meng, Z. Long-Term Effects of Biochar on the Hydraulic Properties of Soil: A Meta-Analysis Based on 1–10 Years Field Experiments. *Geoderma* **2025**, *458*, 117318. https://doi.org/10.1016/j.geoderma.2025.117318.
37. Li, X.; Che, W.; Piao, J.; Li, X.; Jin, F.; Yao, T.; Li, P.; Wang, W.; Tan, T.; Shao, X. Peanut Shell Biochar's Effect on Soil Physicochemical Properties and Salt Concentration in Highly Saline-Sodic Paddy Fields in Northeast China. *BioRes* **2022**, *17*, 5936–5957. https://doi.org/10.15376/biores.17.4.5936-5957.
38. Jin, F.; Piao, J.; Miao, S.; Che, W.; Li, X.; Li, X.; Shiraiwa, T.; Tanaka, T.; Taniyoshi, K.; Hua, S.; et al. Long-Term Effects of Biochar One-off Application on Soil Physicochemical Properties, Salt Concentration, Nutrient Availability, Enzyme Activity, and Rice Yield of Highly Saline-Alkali Paddy Soils: Based on a 6-Year Field Experiment. *Biochar* **2024**, *6*, 40. https://doi.org/10.1007/s42773-024-00332-3.
39. Saifullah; Dahlawi, S.; Naeem, A.; Rengel, Z.; Naidu, R. Biochar Application for the Remediation of Salt-Affected Soils: Challenges and Opportunities. *Sci. Total Environ.* **2018**, *625*, 320–335. https://doi.org/10.1016/j.scitotenv.2017.12.257.
40. Usowicz, B.; Lipiec, J.; Łukowski, M.; Marczewski, W.; Usowicz, J. The Effect of Biochar Application on Thermal Properties and Albedo of Loess Soil under Grassland and Fallow. *Soil. Tillage Res.* **2016**, *164*, 45–51. https://doi.org/10.1016/j.still.2016.03.009.
41. Xiang, Y.; Deng, Q.; Duan, H.; Guo, Y. Effects of Biochar Application on Root Traits: A Meta-analysis. *GCB Bioenergy* **2017**, *9*, 1563–1572. https://doi.org/10.1111/gcbb.12449.
42. Prendergast-Miller, M.T.; Duvall, M.; Sohi, S.P. Biochar–Root Interactions Are Mediated by Biochar Nutrient Content and Impacts on Soil Nutrient Availability. *Eur. J. Soil Sci.* **2014**, *65*, 173–185. https://doi.org/10.1111/ejss.12079.

43. Sharma, P.; Abrol, V.; Shabir, H.; Gupta, S.K.; Gupta, N.K.; Samnotra, R.K.; Chandra, S.; Bashir, O.; Amjid, S.; Singh, P.; et al. Biochar and Anionic Polyacrylamide Modulated Soil Hydraulic Functions Catalyze Water Saving, Root Development and Yield of Basmati Rice. *Front. Plant Sci.* **2025**, *16*, 1660325. https://doi.org/10.3389/fpls.2025.1660325.
44. Olmo, M.; Villar, R.; Salazar, P.; Alburquerque, J.A. Changes in Soil Nutrient Availability Explain Biochar's Impact on Wheat Root Development. *Plant Soil.* **2016**, *399*, 333–343. https://doi.org/10.1007/s11104-015-2700-5.
45. Zou, Z.; Fan, L.; Li, X.; Dong, C.; Zhang, L.; Zhang, L.; Fu, J.; Han, W.; Yan, P. Response of Plant Root Growth to Biochar Amendment: A Meta-Analysis. *Agronomy* **2021**, *11*, 2442. https://doi.org/10.3390/agronomy11122442.
46. Gao, Y.; Shao, G.; Yang, Z.; Zhang, K.; Lu, J.; Wang, Z.; Wu, S.; Xu, D. Influences of Soil and Biochar Properties and Amount of Biochar and Fertilizer on the Performance of Biochar in Improving Plant Photosynthetic Rate: A Meta-Analysis. *Eur. J. Agron.* **2021**, *130*, 126345. https://doi.org/10.1016/j.eja.2021.126345.
47. He, Y.; Yao, Y.; Ji, Y.; Deng, J.; Zhou, G.; Liu, R.; Shao, J.; Zhou, L.; Li, N.; Zhou, X.; et al. Biochar Amendment Boosts Photosynthesis and Biomass in C_3 but Not C_4 Plants: A Global Synthesis. *GCB Bioenergy* **2020**, *12*, 605–617. https://doi.org/10.1111/gcbb.12720.
48. Liu, Z.; Wu, X.; Li, S.; Liu, W.; Bian, R.; Zhang, X.; Zheng, J.; Drosos, M.; Li, L.; Pan, G. Quantitative Assessment of the Effects of Biochar Amendment on Photosynthetic Carbon Assimilation and Dynamics in a Rice–Soil System. *New Phytol.* **2021**, *232*, 1250–1258. https://doi.org/10.1111/nph.17651.
49. Schmidt, H.; Kammann, C.; Hagemann, N.; Leifeld, J.; Bucheli, T.D.; Sánchez Monedero, M.A.; Cayuela, M.L. Biochar in Agriculture—A Systematic Review of 26 Global Meta-analyses. *GCB Bioenergy* **2021**, *13*, 1708–1730. https://doi.org/10.1111/gcbb.12889.
50. Joseph, S.; Cowie, A.L.; Van Zwieten, L.; Bolan, N.; Budai, A.; Buss, W.; Cayuela, M.L.; Graber, E.R.; Ippolito, J.A.; Kuzyakov, Y.; et al. How Biochar Works, and When It Doesn't: A Review of Mechanisms Controlling Soil and Plant Responses to Biochar. *GCB Bioenergy* **2021**, *13*, 1731–1764. https://doi.org/10.1111/gcbb.12885.
51. Ye, L.; Camps-Arbestain, M.; Shen, Q.; Lehmann, J.; Singh, B.; Sabir, M. Biochar Effects on Crop Yields with and without Fertilizer: A Meta-analysis of Field Studies Using Separate Controls. *Soil. Use Manag.* **2020**, *36*, 2–18. https://doi.org/10.1111/sum.12546.

Disclaimer/Publisher's Note: The statements, opinions and data contained in all publications are solely those of the individual author(s) and contributor(s) and not of MDPI and/or the editor(s). MDPI and/or the editor(s) disclaim responsibility for any injury to people or property resulting from any ideas, methods, instructions or products referred to in the content.